

Technique for localization of degraded cable insulation regions using TDR measurement artifacts

Ruslan Papazyan
 Faculty of Electrical Engineering
 Technical University of Sofia
 Sofia, Bulgaria
 rpapazyan@tu-sofia.bg

Abstract—Time Domain Reflectometry (TDR) is a method suitable for localizing changes in impedance changes along a transmission line. TDR is used for identifying regions along medium voltage cables affected by water treeing. This was made possible by utilizing the non-linear characteristics of water trees in order to separate reflections from geometric cable variations and those from insulation changes. The possibility to detect local changes in the velocity of wave propagation has been presented as a technique for localization of insulation ageing.

Key words—Crosslinked polyethylene insulation, power cables, time domain reflectometry, transmission line discontinuities, trees (insulation), localization, condition monitoring.

I. INTRODUCTION

WATER TREEING is a known phenomenon that can reduce the breakdown strength of cross-linked polyethylene (XLPE) insulated cables. In a series of studies [...] it has been shown that water trees can be detected through measurements of the frequency dependent dielectric parameters measurements, also referred to as *dielectric spectroscopy*. Considering that dielectric spectroscopy evaluates the cable insulation condition as a whole, while water trees are a local phenomenon, further studies and techniques were developed for localization of the water treed region [1]. These techniques were based on TDR and can detect local insulation changes along the cable during, or after application of operating high voltage levels. These techniques aim to distinguish the reflections from geometrical irregularities and other measurements artifacts from the ones originating from insulation changes caused by water-treeing.

The focus of this paper is to present a measurement technique that utilizes these measurement artifacts in order to identify local changes in the speed of wave propagation along the cable length. These velocity changes are used as indication for water-tree insulation ageing.

II. HIGH FREQUENCY CABLE CHARACTERISTICS

Describing a power cable as a transmission line introduces the unit length inductance (L), capacitance (C), resistance (R) and conductance (G). The frequency dependent propagation constant (γ) and characteristic impedance (Z_c) can be

presented as

$$\gamma(\omega) = \alpha + j\beta = \sqrt{(R + j\omega L)(G + j\omega C)} = \sqrt{zy}$$

$$Z_c(\omega) = \sqrt{\frac{R + j\omega L}{G + j\omega C}} = \sqrt{\frac{z}{y}} \quad (1)$$

where z and y are the series impedance and shunt admittance, respectively. α and β are the attenuation and phase constants, where β defines the phase velocity v (m/s) as

$$v = \omega / \beta = 2\pi f / \beta \quad (2)$$

Fig. 1 presents are medium voltage (MV) power cable design. In this paper a cable model is used for analysis where the conductor screens and the XLPE insulation constitute the shunt admittance of the model. The admittance of each insulation/screen layer is given by its complex capacitance C^* , determined by the geometric capacitance C_0 and the complex permittivity ϵ^* , i.e.

$$y = j\omega C^*(\omega) = j\omega C_0 (\epsilon'(\omega) - j\epsilon''(\omega)) \quad (3)$$

where $\epsilon'(\omega)$ and $\epsilon''(\omega)$ are the capacitive and loss part, respectively, of the complex permittivity.

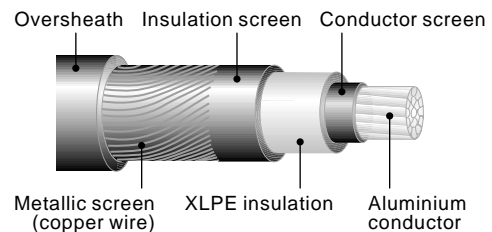


Fig. 1. MV power cable design.

III. CONCEPT FOR LOCALIZATION OF INSULATION DEGRADATION

A. Water tree voltage dependent non-linearity

To distinguish in the TDR measurement between the

reflections from water-tree degradation and other geometric changes one can use the voltage dependent non-linearity of water trees, Fig. 2. [2]. This implies that observed changes in the insulation before and after voltage application, alternatively observed by comparing measurements at 0° and the top 90° of the applied voltage, Fig. 3., can be attributed to water treeing.

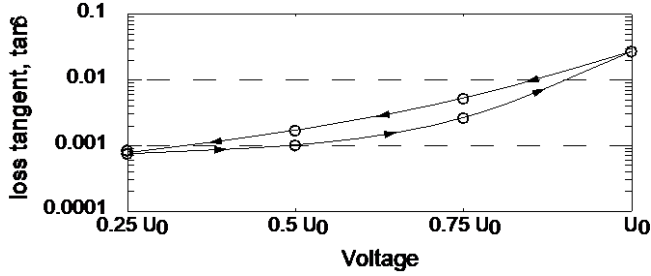


Fig. 2. An example of $\tan\delta$ measurements on a cable significantly affected by water treeing. Repeated measurements at the same voltage levels shows a hysteresis effect. [2]

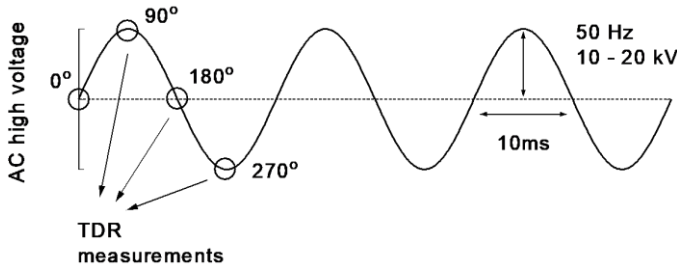


Fig. 3. Illustration on the possibility to perform TDR during application of AC operating voltages and compare data measured at 0° and the top 90° of the applied voltage. [2]

IV. SENSITIVITY STUDIES

When localizing changes in $\varepsilon(\omega)$ the feasibility of detecting these insulation variations must be assessed.

For the purpose the effects of changes in ε' and ε'' on $\gamma(\omega)$ and $Z_c(\omega)$ are simulated using a cable model described in [3]-[5]. Only $\varepsilon(\omega)$ of the XLPE insulation layer is varied for the purpose of this investigation. Fig. 4 (a) shows the effect of 5% change in ε' on the cable wave propagation properties, where both $\gamma(\omega)$ and $Z_c(\omega)$ are affected.

The reflection caused by the impedance change is deduced from the reflection coefficient

$$\Gamma = \frac{(Z_c^* - Z_c^0)}{(Z_c^* + Z_c^0)} \quad (4)$$

giving the relation between the changed (Z_c^*) and initial cable impedance (Z_c^0).

A change in ε'' , on the other hand, affects primarily the attenuation of the propagating signal, Fig. 4 (b). A TDR measurement, based on the concept of detecting reflections caused by changes in the characteristic impedance, would therefore be insensitive to ε'' variations.

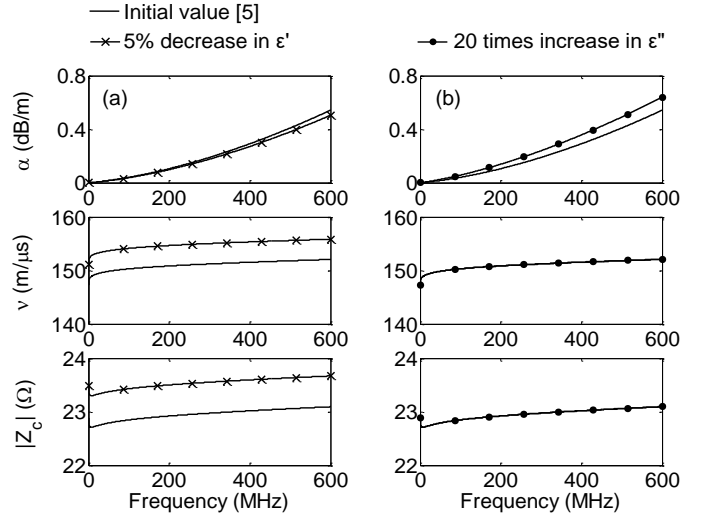


Fig. 4. Effect on the cable parameters $\gamma(\omega)$ and $Z_c(\omega)$ of changes in ε' and ε'' in the XLPE insulation.

A. Localization of $\varepsilon'(\omega)$ changes by TDR

The effects of $\varepsilon'(\omega)$ changes are also simulated in the time domain to demonstrate how the insulation variations can be localized by TDR measurements. The propagation of a Gaussian pulse with amplitude of 1 and 50 ns pulse-width is studied in this investigation.

Fig. 5. shows a simulation result where $\varepsilon'(\omega)$ of the XLPE layer along 1/3 of the cable length is decreased by 5%. That change corresponds to a 2.5% increase in Z_c (Fig. 4 (a)) or using eq. (4) the reflection coefficient is calculated at $\Gamma = 0.0123$, Fig. 5 (b).

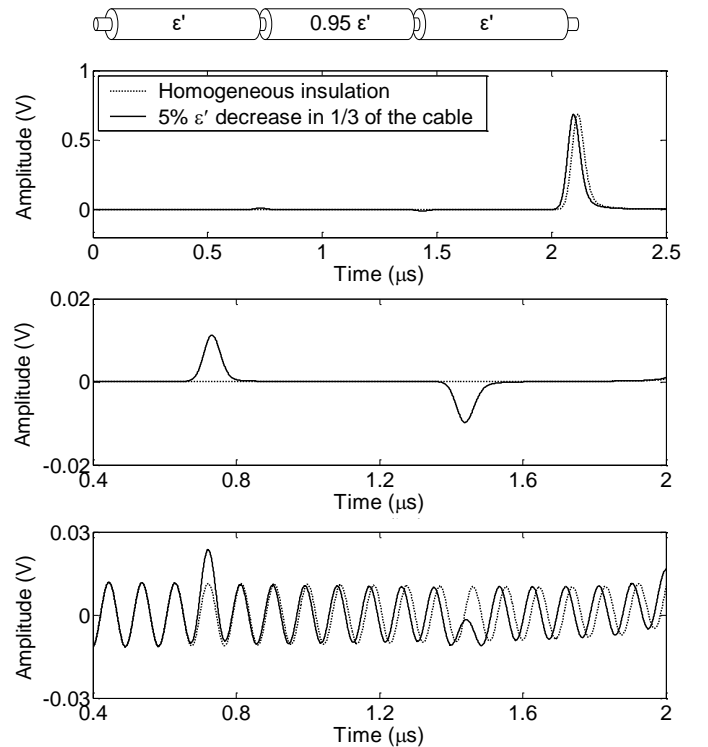


Fig. 5. Simulation of TDR signal in a cable with $\varepsilon'(\omega)$ changed in 1/3 of its length. The integrated effect of velocity change can be seen in the shift in time of arrival of the reflection at 2 μ s (open end reflection).

The reflection caused by the impedance change would be attenuated as it propagates along the cable and the ability to

detect it would diminish with the distance of the impedance change from the measuring end. Furthermore, pulse generator (PG) instabilities, sporadic signals and other artifact, unrelated to the cable geometry, can reduce the ability to detect and localize insulation related reflections, even if the differential TDR technique is applied.

A new localization concept is therefore investigated which uses the fact that a change in $\varepsilon'(\omega)$ will equally affect $Z_c(\omega)$, as well as the velocity $v(\omega)$. The effects of $v(\omega)$ variations can be observed in the open end reflection, where a shift in the arrival time is present, Fig. 5 (a). The difference in the propagation time can be calculated using the relation

$$\Delta t = t_* - t_0 = \int_0^{l_*} \frac{dl}{v_*} - \int_0^{l_0} \frac{dl}{v_0} \quad (5)$$

where t_0 and t_* denote the propagation time over the homogeneous cable and one with insulation changes in a section of length (l_*), respectively. For the presented case this change is calculated at $\Delta t = 0.0163 \mu\text{s}$.

Assuming that the reflections caused by the impedance change are undetectable, the $\varepsilon'(\omega)$ change would be noted by the shift of the reflection from the open end. However, without the ability to detect reflections, the cause of the shift but would be unlocalizable using the classical TDR approach.

A key feature in this case is utilizing the reflections from the cable irregularities. These reflections could be significantly larger than the anticipated signals from insulation changes and the ability to measure these is considerably improved. Then using them as a reference one can detect the location from where the changes in the velocity start to take place, Fig. 5 (c). In the first unaffected by changes section (up to $0.7 \mu\text{s}$) no shifting can be observed in the reflections from the repetitive geometrical irregularities. These reflections would consistently shift when propagating in the affected by the change region ($0.7 - 1.5 \mu\text{s}$) and the time shift would remain constant in the following unaffected insulation ($1.5 - 2 \mu\text{s}$).

B. Effect of insulation and conductor screen changes on the TDR measurements

If the concept is based on the idea of inducing changes by the application of high voltages, it is reasonable to assume that the semi-conducting materials can also be affected by these voltage stresses. Therefore, the effect of semicon changes on the TDR propagation is also studied. Fig. 6 shows the results of signal propagation along a cable where the complex permittivity of the semicon layers has been altered.

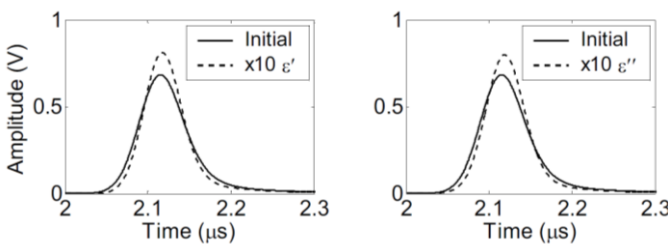


Fig. 6. Simulating the effect of insulation and conductor screen changes on the TDR measurements.

It could be observed that the change is predominantly affecting the attenuation of the signal, but not the velocity of its propagation. It could therefore be concluded that a change in the propagation speed can be attributed to a $\varepsilon'(\omega)$ change in the bulk of the XLPE insulation. It is noteworthy that changes in the insulation/conductor screens and effects on the TDR measurements from e.g. the surrounding medium mainly affect the attenuation. They have limited influence on the speed of wave propagation [6]

V. MEASURING SYSTEM

A system has been designed for TDR measurements during the application of high AC voltages, Fig. 7., has been described in detail in [2]. This systems allows to perform TDR measurements both before and after, as well as during high voltage application.

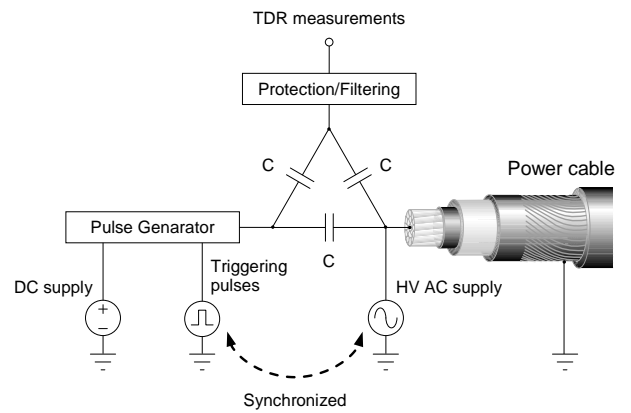


Fig. 7. TDR system for phase-locked measurements during the application of high AC voltages [...].

VI. LOCALIZING VARIATIONS IN $v(\omega)$

Two cable objects were investigated as part of a previous study [2]. In this study focused on the concept of localization of $\varepsilon'(\omega)$ changes by TDR measurements utilizing reflections caused by the change in $Z_c(\omega)$. Using this approach water treed cable sections were localized only for one of the cable samples (Cable 1). However, verification measurements, using dielectric spectroscopy and subsequent destructive water tree analysis, revealed insulation deterioration the second (Cable 2) measurement object as well.

This outcome initiated additional studies and the development of a new concept for localization of local velocity variations in $v(\omega)$, which are indicative of respective insulation changes

Fig. 8 shows TDR measurements on the Cable 2 measurement object, which is 170 m long XLPE cable rated at 24 kV. Parts of Cable 2 marked with A had approximately 30-years in operation and parts marked with B – around 10 years. TDR measurements were performed from both cable ends.

The effect of water tree changes on the speed of wave propagation can be observed in the time shift of the open end reflection (at $2.4 \mu\text{s}$). Changes in the signal damping can also be detected.

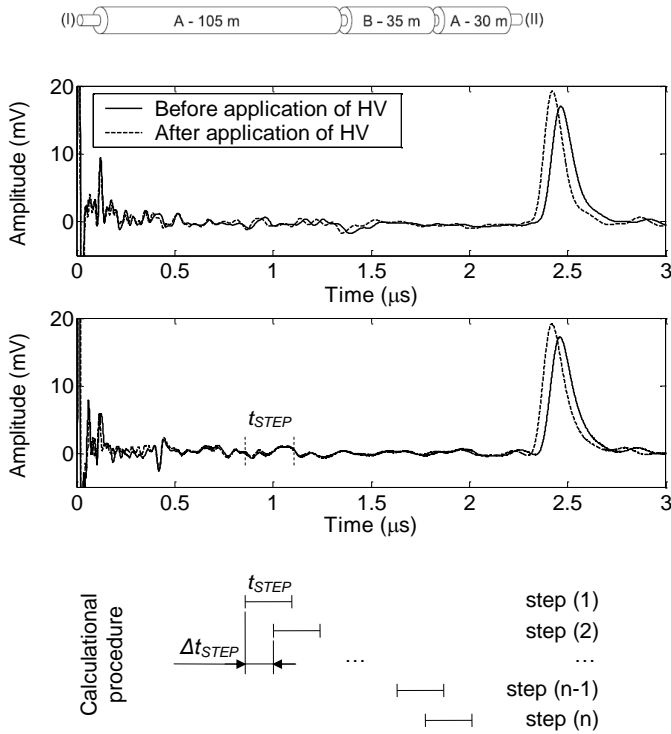


Fig. 8. TDR measurements on Cable two performed from both cable ends.

The decrease in attenuation is however greater than the expected velocity change, corresponding to the same ϵ' variation, Fig. 4. Semicon layer changes and other measurement influences are suggested to additionally affect the signal damping.

To assist the localization of the section(s) that caused the observed shift a calculation procedure is used, Fig. 8 *bottom diagram*. Initially corresponding sections of the measured signals before, $u_b(t_b)$, and after, $u_a(t_a)$, the application of HV are chosen with a length t_{STEP} . It is then estimated how much $u_a(t_a)$ is shifted in time as compared to $u_b(t_b)$ by using the relation between the two time bases $t_a = k_t t_b$. The value of k_t is obtained by an optimization procedure minimizing the relation

$$\min_{\{k_t\}} \sum_{i=1}^n \left(\frac{u_{b,i}(t_{b,i}) - u_{a,i}(k_t t_{a,i})}{u_{b,i}(t_{b,i}) + d} \right)^2 \quad (6)$$

where n is the number of sample points contained in the section t_{STEP} . d is a damping coefficient introduced to improve the numerical conditioning of the division when $u_b \approx 0$.

A second section is then chosen, shifted from the first one by an amount Δt_{STEP} ($\Delta t_{STEP} \leq t_{STEP}$), and the same optimization procedure repeated. This iterative process is used until the entire measured signal is covered. As a result the coefficient $k_t(t_b)$ is calculated as a function of the propagation time t_b , and thereby also as a function of the cable length l ($t_b = \int dl/v_b$). Fig. 9 shows an example of the k_t profile and its dependence on the choice of Δt_{STEP} .

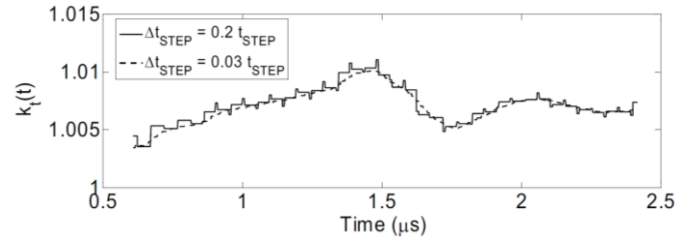


Fig. 9. Profile of the coefficient $k_t(t)$ and its dependence on the choice of Δt_{STEP} . Example of measurements from side (I) on Cable 2.

The velocity profile after the voltage application (v_a) can then be calculated using again the relation $t_a = k_t(l)t_b$, i.e.

$$\int_0^l \frac{dl}{v_a(l)} = k_t(l) \int_0^l \frac{dl}{v_b(l)} \Rightarrow \frac{1}{v_a} = \frac{1}{v_b} k_t(l) + t_b \frac{dk_t(l)}{dl} \quad (7)$$

Identical approach is utilized for velocity change localization during the application of HV, where the measurements at the zero crossing (0°) and at the top (90°) of the HV substitute $u_b(t_b)$ and $u_a(t_a)$, respectively. An important difference should be noted as compared to the measurements before and after the application of HV. While in the first case the entire TDR signal is influenced after the application of the high voltage, in the on-line case only signals with frequency content above approximately 20 MHz are affected, Fig. 10.

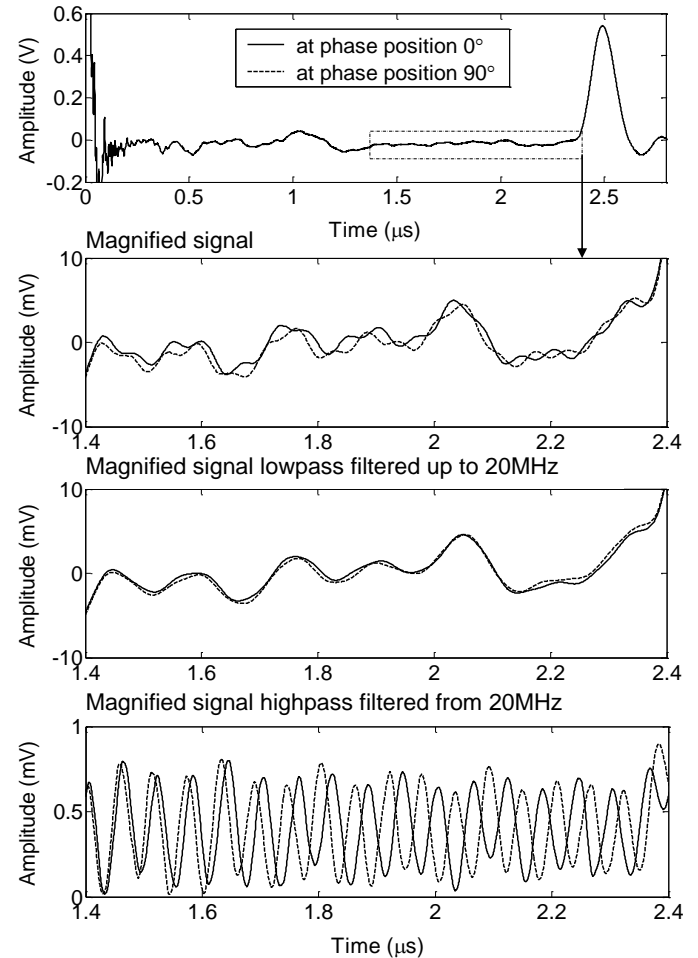


Fig. 10. TDR measurements at 0° and 90° of the HV AC (Cable 2, side II). Measurements are performed at 10 Hz and $0.5U_0$. The HV level is chosen to avoid discharges at the interface between the measuring system and power cable. Time shift can only be observed for frequencies above 20 MHz.

Using the above mentioned measurement techniques the local velocity profile has been measured for Cable 2, Fig. 8. The velocities changes after the application of high voltages and at 90° of the applied HV have been compared. Fig. 11 shows an even increase in the velocity in the water-treed section, while the speed in the new section is least affected, where the initial speed is $v = 147 \text{ m}/\mu\text{s}$. The change in the local velocity of wave propagation corresponds to a ϵ' change of 7%.

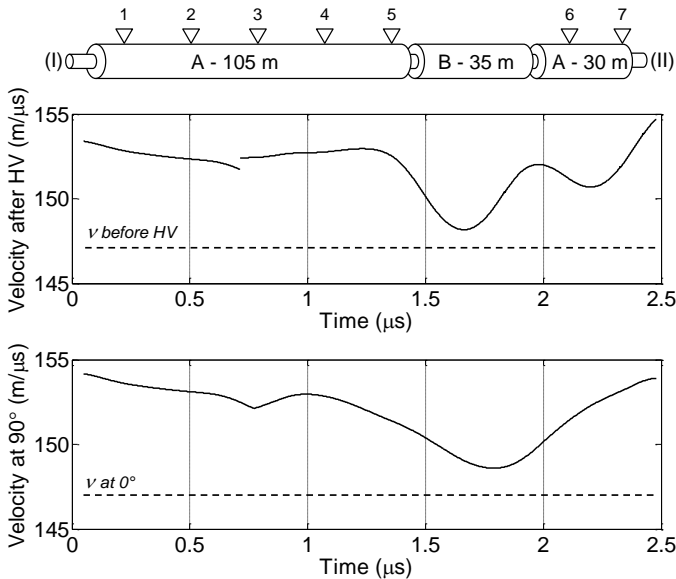


Fig. 11. Local velocity profiles based on measurements before, after and at 0° and 90° of the applied HV. Measurements from both sides are performed, with results from 0.7 to $2.5 \mu\text{s}$ measured from side I and from 0 to $0.7 \mu\text{s}$ – from side II.

VII. CONCLUSIONS

Nondestructive diagnostic techniques have been presented for the localization of water-tree deteriorated sections along medium-voltage power cables. It was shown that the $v(\omega)$ variations are least susceptible to measurement artifacts. When a short cable section is affected by water treeing, the only observable effect would be the reflections caused by the $Z_c(\omega)$ change. For longer deteriorated sections, even if no reflections are localizable, the effect of $v(\omega)$ change is integrated over the length and a shift can be observed in the time of arrival at the open end reflection. Using signal processing it can then be investigated if the shift is caused by local water tree degradation and localize its position. A key feature for the signal processing is using as reference the reflections from geometrical irregularities along the cable.

ACKNOWLEDGMENT

The authors would like to thank the Research and Development Sector at the Technical University of Sofia for the financial support.

The author would like to thank Prof. R. Eriksson, Prof. U. Gäfvert and Prof. P. Nakov for their academic support.

REFERENCES

[1] Björn Holmgren, Dielectric Response, Breakdown Strength and Water Tree Content of Medium Voltage XLPE Cables, Tech. Lic., Royal Institute of Technology (KTH), TRITA-EEA-9705, Stockholm, Sweden, 1997.

[2] R. Papazyan, Concepts for market-based MV cable operations and maintenance using insulation parameters measurements (2020) 12th Electrical Engineering Faculty Conference, BuIEF 2020, art. no. 9326055, DOI: 10.1109/BuIEF51036.2020.9326055

[3] P. Werelius, P. Thäming, R. Eriksson, B. Holmgren and U. Gäfvert, "Dielectric Spectroscopy for Diagnosis of Water Tree Deterioration in XLPE Cables", *Diel. And El. Ins., IEEE Trans. on*, vol. 8, 27–42, February 2001.

[4] R. Papazyan, P. Pettersson, H. Edin, R. Eriksson, U. Gäfvert, "Extraction of the High Frequency Power Cable Characteristics from S-parameter Measurements," *Diel. and El. Ins., IEEE Trans. on*, Vol. 11, 461-470, June 2004.

[5] G. Mugala, R. Eriksson, U. Gäfvert, P. Pettersson, "Measurement technique for high frequency characterization of semi-conducting materials in extruded cables," *Diel. and El. Ins., IEEE Trans. on*, vol. 11, 471-480, June 2004.

[6] R. Papazyan, D. Pommerenke, R. Eriksson, "Modeling the Wave Propagation Properties of Power Cables Using Numerical Simulations", *CPEM 2004*, London, UK, June 27- July 2 2004, pp. 412-413.